ELSEVIER

www.elsevier.nl/locate/jorganchem

Journal of Organometallic Chemistry 590 (1999) 7–14

Journal of Organometallic Chemistry

Synthesis, structure and spectroelectrochemistry of bis(η^6-1,4-tri-*tert*-butyl-benzene)chromium(0) and bis(η^5-1,2,4-tri-*tert*-butyl-cyclopentadienyl)cobalt(II). Dia- and paramagnetic sandwich complexes derived from sterically highly demanding π-ligands

Jörg J. Schneider [a,*], Norbert Czap [a], Dirk Spickermann [a], Christian W. Lehmann [b], Marco Fontani [c], Franco Laschi [c], Piero Zanello [c]

[a] *Institut für Anorganische Chemie der Universität GH-Essen, Universitäts-straße 5–7, D-45117 Essen, Germany*
[b] *Max-Planck-Institut für Kohlenforschung, Kaiser-Wilhelm-Platz 1, D-45470 Mülheim an der Ruhr, Germany*
[c] *Dipartimento di Chimica, Università di Siena, Pian dei Mantellini 44, I-53100 Siena, Italy*

Received 6 May 1999; received in revised form 24 May 1999

Abstract

Metal atom synthesis gives access to the bis(arene)chromium sandwich of 1,4 di-*tert*-butyl-benzene (**5**). **5** displays an axial sandwich structure with a linear arene–chromium–arene axis and a Cr–arene distance of 1.64 Å. Reduction of [{(η^5-1,2,4 tri-*tert*-butyl-Cp)CoCl}$_2$] with the trianion of decacyclene in THF produces the cobaltocene sandwich [(η^5-1,2,4 tri-*tert*-butyl Cp)$_2$Co] **2** as black crystals in 65% yield. Electrochemistry shows that the monocations **2**$^+$ and **5**$^+$ are able to support reversibly the one-electron reduction to their corresponding neutral congeners. © 1999 Elsevier Science S.A. All rights reserved.

Keywords: Sandwich complexes; Chromium; Cobalt; Electrochemistry; Metal atoms

---

1. Introduction

Different synthetic methodologies have been developed for the synthesis of bis(arene) sandwich complexes. The classical approach to these group of compounds, the wet chemical reducing Fischer–Hafner synthesis, has the major drawback of arene isomerization, due to usage of the strong Lewis acid $AlCl_3$ as a reducing agent and therefore failing to produce pure bis(η^6-alkylbenzene)chromium sandwich complexes [1]. The most widely applicable method for the synthesis of this class of compounds is the metal vapor synthesis technique, which has been explored for a wide range of homoleptic, binary as well as mixed bis(η-arene)metal complexes, and provides a straightforward direct approach starting from metal atoms and the appropriate arene [2]. Up to now alkyl-substituted benzenes can only be introduced as ligands in such complexes by the metal vapor approach leading to isomeric pure products. The sterically highly demanding 1,3,5-tri-*tert*-butylbenzene ligand has already demonstrated its ability to sandwich one or even two chromium atoms in bis(arene) type complexes or (arene)$_3$Cr$_2$ triple decker complexes [3]. Interestingly no binary chromium sandwich complexes of the sterically, nevertheless less encumbered 1,4-bis-*tert*-butyl-benzene ligand are known so far.

In contrast to the bis(η^6-alkylbenzene)chromium sandwich complexes, bis(η^5-alkyl-cyclopentadienyl)-cobalt complexes are accessible by various classical wet chemical routes in isomeric pure form. The co-condensation route between Co atoms and differently substituted cyclopentadiene ligands, typically, does not lead to the formation of bis(η^5-Cp^R)Co complexes. Instead, mixed (η^5-Cp^R)(η^4-cyclopentadiene)Co com-

---

* Corresponding author. Tel.: +49-201-1832413; fax: +49-201-1834195.
E-mail address: joerg.schneider@uni-essen.de (J.J. Schneider)

PII: S0022-328X(99)00383-6

plexes are formed in metal atom reactions between Co atoms and these ligands [4]. To the best of our knowledge the synthesis of [(η^5-1,3-di-*tert*-butyl-Cp)$_2$Co] **1** is the only case in which formation of a [(η^5-Cp^R)$_2$Co] sandwich was reported from reaction of Co atoms and a cyclopentadiene ligand [5]. **1** displays a skewed sandwich structure in which both 1,3-di-*tert*-butyl Cp rings are slightly tilted by 9(1)° to one another with respect to an ideal axial (η^5-Cp^R)–M–(η^5-Cp^R) sandwich arrangement. This distortion can either be understood by the sterically encumbered situation impinged on the complex by the four bulky *tert*-butyl ligands, which may force the complex to crystallize with a nonlinear (η^5-Cp^R)–Co–(η^5-Cp^R) arrangement, or by crystal packing forces, resulting in a sandwich arrangement with a skewed (η^5-Cp)–Co–(η^5-Cp) axis [5]. Okuda could show that [1^+] [PF_6^-] displays a barrier towards ring rotation of $\Delta G^{\ddagger} = 12.6$ kcal mol^{-1} [6].

In co-condensation experiments between Co atoms and the sterically highly demanding 1,2,4-tri-*tert*-butyl-Cp ligand, we did not observe formation of a related bis(η^5-Cp^R)Co sandwich complex [5]. We attribute this to the incompatibility of the steric demands of the 1,2,4-tri-*tert*-butyl-Cp ligands and the necessary inter-ring sandwich distance to realize a linear or a skewed (η^5-Cp^R)–Co–(η^5-Cp^R) bonding mode which results in formation of the (so far unknown) Co sandwich complex bis(η^5-1,2,4-tri-*tert*-butyl-Cp)cobalt **2** with six *tert*-butyl groups. This situation could well account for the fact that in general only scattered reports describing sandwich-type complexes of this ligand are known. However, reports on the existence of the sterically highly encumbered hexakis(trimethylsilyl) cobaltocenium sandwich ion by Okuda [7] (see Scheme 1) and recent reports by Sitzmann on metallocene sandwich complexes of Bi [8] **3** and Mn [9] **4** bearing the 1,2,4-tri-*tert*-butyl-Cp ligand prompted us to look into the synthesis and redox behavior of the bis(η^5-1,2,4-tri-*tert*-butyl-Cp)cobalt sandwich complex (**2**) more closely. Herein we report on our findings towards synthesis, structure and spectroelectrochemistry of bis(η^5-1,2,4-tri-*tert*-butyl-Cp)Co(I,II) (**2**) using the trianion of the polycondensed hydrocarbon decacyclene as reductant, as well as of the bis(arene)chromium complex pair bis(η^6-1,2,4-tri-*tert*-buytl-benzene)Cr(0,I) (**5**$^{0/+}$), which is accessible by metal vapor synthesis and electrochemical oxidation.

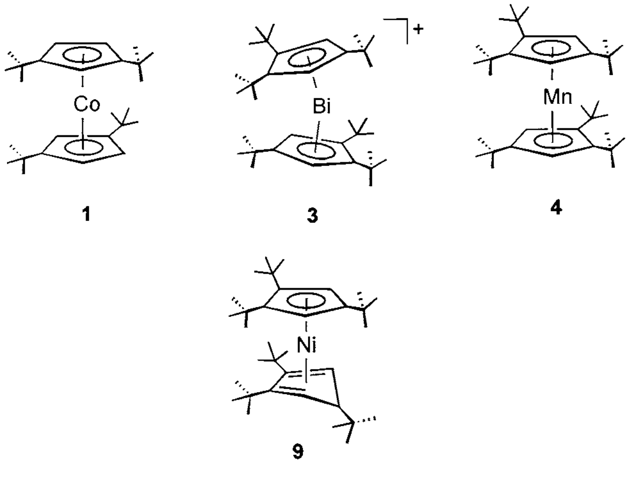

Scheme 1.

2. Results and discussion

2.1. Synthesis of (η^6-1,4-di-tert-benzene)chromium(0) 5

When a nearly three-fold molar excess of 1,4-di-*tert*-butyl-benzene vapor is co-condensed with thermally generated chromium vapor at −196°C during 2 h, a brownish–green co-condensate formed. After workup and removal of solvent and excess ligand by sublimation, the remaining crude material can be sublimed at 130°C/10^{-2} Pa giving **5** as an olive green analytical pure microcrystalline solid (Eq. (1))

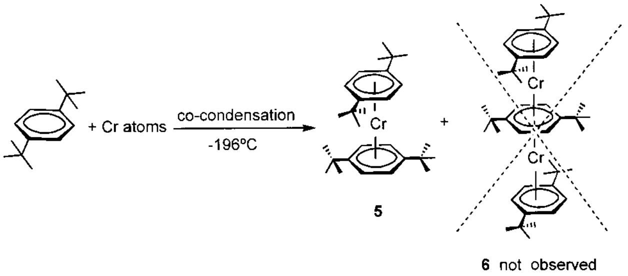

(1)

Despite our careful sublimation procedure, no residual organometallic material remained after **5** was completely sublimed from the crude co-condensation product. This fact is important with respect to the formation of a triple decker complex **6**, which might be a possible higher nuclearity product formed in addition to the sandwich complex **5**, under the experimental conditions (viz. low ligand to metal ratio) chosen in our experiment. It is known that such triple decker complexes do form under moderate ligand excess with multiple alkyl-substituted arenes like 1,3,5 trimethylbenzene [10] or 1,3,5 tri-*tert*-butyl-benzene [3] as side products in co-condensation experiments between chromium atoms and these ligands.

2.2. Spectroscopic characterization of bis (η^6-1,4-di-tert-benzene)chromium(0) 5

Spectroscopic characterization of **5** by MS and ^{1}H-NMR spectroscopy is straightforward. In the EI-MS, the molecular ion appears at 432. Base signal is the half sandwich with *m*/*e* 242.

NMR: as for all alkylsubstituted bis(arene) sandwich complexes, **5** is very prone to air oxidation and therefore NMR samples, even when prepared under vigorous air-free conditions in predried and degassed solvents, show only broad unresolved ^{1}H-NMR signals due to a fast electron exchange between stable paramagnetic bis(arene)chromium species $\mathbf{5}^{+\cdot}$ formed by oxidation during sample preparation, and the neutral bis(arene)-chromium complex **5**. This causes a severe line broadening. A concentration of 10^{-6} M of $\mathbf{5}^{+\cdot}$ is sufficient to observe this effect quite dramatically [11]. If the arene ring ligands bear proton-containing substituents, the same effect is observed, albeit the broadening of these signals compared with the ones bound to the arene moiety is proportional to the spin density of the unpaired electron at these positions. Thus the number of σ-bonds separating the paramagnetic Cr(I) center from the ^{1}H-nucleus is decisive for that line broadening if one assumes a spin density transfer mechanism mediated mainly by the σ-bonding framework [12,13]. Therefore the ^{1}H-NMR line broadening due to this paramagnetic exchange is expected to be much more pronounced for the four aromatic protons of **5** compared with the protons of the *tert*-butyl substituents bound in the vicinity of this sandwich.

Mainly due to different spin-exchange processes in ^{1}H- and ^{13}C-NMR spectroscopy for bis(arene)chromium complexes, this is not the case for the ^{13}C-spectrum of **5**, which shows well-resolved, sharp peaks at δ (ppm) = 101.7 (=C*t*-Bu), 73.4 (=CH), 34.4 ($-C(CH_3)_3$) and at 32.1 ($-C(CH_3)_3$), consistent with a symmetrical bis(arene) sandwich structure.

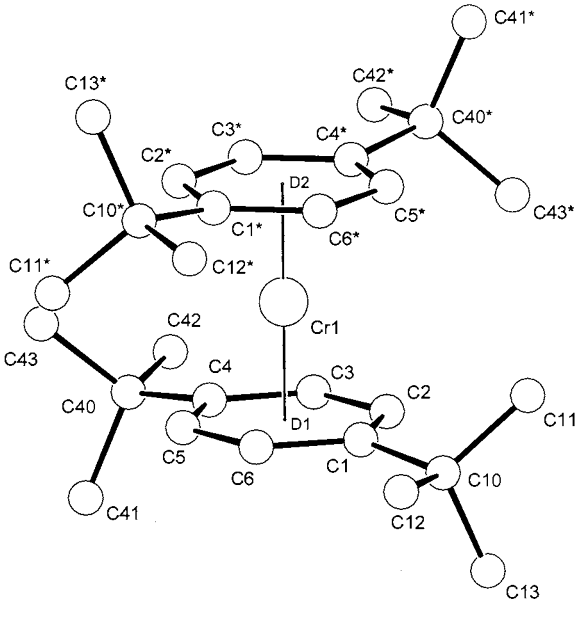

Fig. 1. Molecular structure of **5** in the solid state. Selected bond lengths [Å]: Cr–C1 2.181(3), Cr–C2 2.149(3), Cr–C3 2.159(3), Cr–C4 2.193(3), Cr–C5 2.157(3), Cr1–C6 2.154(3).

The same sample, however, gives a ^{1}H-NMR spectrum with very broad signals due to the presence of the thermally robust $\mathbf{5}^+$ radical species besides neutral **5**. However, prolonged thermal treatment (120°C/24 h) of the NMR sample of **5** containing such traces of $\mathbf{5}^+$ produces a well-resolved spectrum with signals at δ (ppm) = 4.44 (s, 8H, =CH) and 1.34 ppm (s, 36H, *tert*-Bu), and a signal half width < 5 Hz, indicating complete decomposition of the paramagnetic radical species $\mathbf{5}^+$.

2.3. Molecular structure of [(η^6-1,3-di-*tert*-butylbenzene)$_2$Cr] 5

Suitable single crystals of **5** were obtained from a concentrated toluene solution at −30°C. Its molecular structure is depicted in Fig. 1.

5 displays the typical η^6-sandwich structure and exhibits exact (crystallographic) C_2 symmetry intersecting the molecule at the chromium atom parallel to the arene rings. The 1,4-di-*tert*-butylbenzene ligand is coordinated in such a way that the projection of the arene ring centroid coincides with the chromium atom, affording a linear (180.0°) ligand–metal–ligand arrangement that is not symmetry imposed. The chromium ring centroid distance is 1.640 Å. The co-planar arene ligands are oriented in a staggered fashion, the twist angle being 83°. The ring bond angles at each *ipso* carbon atom are reduced to 117° (C6–C1–C2 and C3–C4–C5) while the four *tert*-butyl substituents are bent out of the plane of the essentially planar arene rings by 0.18 Å (6.5°) away from the chromium atom, in order to reduce the steric crowding. The repulsion of the *tert*-butyl substituents does not lead to an increased Cr–C bond length; 2.166(3) Å in **5** compared to 2.221(5) for Cr–C in other bis(η^6-arene) compounds [15].

2.4. Crystal data for 5

$C_{28}H_{44}Cr$, Mr = 432.63, orthorhombic, space group *Pbcn* (no. 60), $a = 11.957(2)$, $b = 16.835(3)$, $c = 11.962(2)$ Å, $V = 2408.4(8)$ Å^3, $Z = 4$, $D_{\text{calc.}} = 1.193$ Mg m^{-3}, $\mu(\text{Mo-K}_\alpha) = 0.487$ mm^{-1}, $F(000) = 944$, $T = 90(1)$ K, block-shaped crystal $0.35 \times 0.49 \times 0.65$ mm. Data were collected on a Nonius Mach3 diffractometer using Mo–K$_\alpha$ ($\lambda = 0.71073$ Å) radiation. The cell parameters were determined by least-squares refinement of diffractometer angles for 25 reflections with $22.22 \leq \theta \leq 23.99°$. A total of 8083 reflections within $1.21 \leq \theta \leq 27.43°$ were collected and merged into 2918 unique reflections ($R_{\text{int}} = 5.9\%$) of which 2507 had intensities $> 2\sigma(I)$. The crystal structure was solved using direct methods (SHELXS-86) [14a] and refined by full-matrix least-squares based on F^2 (SHELXS-93) [14b] using all reflections and 141 refined variables. All non-hydrogen atoms were refined anisotropically, hydrogen atoms were located from difference Fourier maps and constrained to idealised positions. Complete structure refinement required the inclusion of a 24% twin component (pseudo tetragonal, twin law 0 0 1, 0 −1 0, 1 0 0). Further, the residual electron density contained evidence of another crystal component with the chromium atom located at x, $\approx y + 1/2$, z and a site occupancy of 0.03. The least-squares refinement converged at R_1 and wR_2 values of 0.057 and 0.163 with a goodness-of-fit parameter of 1.13.

2.5. Synthesis of [(η^5-1,2,4 tri-tert-butyl-Cp)$_2$Co] **2**

It is well known that polycondensed aromatics form stable polyanions with a high reducing power in homogeneous solution. Herein we employed the trianion of decacyclene **8**, which is formed by reduction of the hydrocarbon with three equivalents of potassium metal [16] to reduce the bridged Co dimer [{(η^5-1,2,4 tri-*tert*-butyl-Cp)CoCl}$_2$] **7** [17] in homogeneous THF solution under mild conditions at −78°C. This produced a deep brown solution from which after workup and crystallization black crystals of the sandwich complex **2** were isolated in 65% yield (Eq. (2)). To the best of our knowledge this is the first report that the trianion of decacyclene can be successfully employed for the synthesis of bis(arene) complexes.

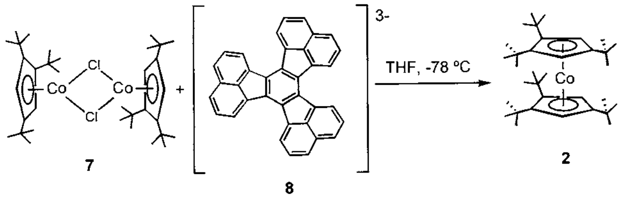

(2)

2.6. Spectroscopic characterization of [(η^5-1,2,4-tri-tert-butyl Cp)$_2$Co] **2**

MS analysis of **2** displayed the molecular ion as base peak (100%) at *m*/*e* 525. All other fragment ions are below 10%.

In accord with the bis(η^5-Cp^R) coordination mode, **2** has one electron in excess to 18 e and therefore displays low-field-shifted paramagnetic NMR signals in a 2:1 overall intensity ratio at $\delta = 3.47$ ($\nu_{1/2} = 54.8$) and 3.65 ($\nu_{1/2} = 27$ Hz) ppm compared to diamagnetic sandwich complexes of this ligand, e.g. **9** [18]. Signals of the remaining four protons at the Cp ring ligands are not observed due to paramagnetic broadening.

2.7. Spectroelectrochemistry (CV and coupled EPR measurements) of [(η^5-1,2,4 tri-tert-butyl Cp)$_2$Co] **2** *and [{(η^6-1,4 di-tert-butylbenzene)$_2$Cr]* **5**

Fig. 2 depicts the electrochemical behavior of the two monocations **2**$^+$ and **5**$^+$ in dichloromethane solution.

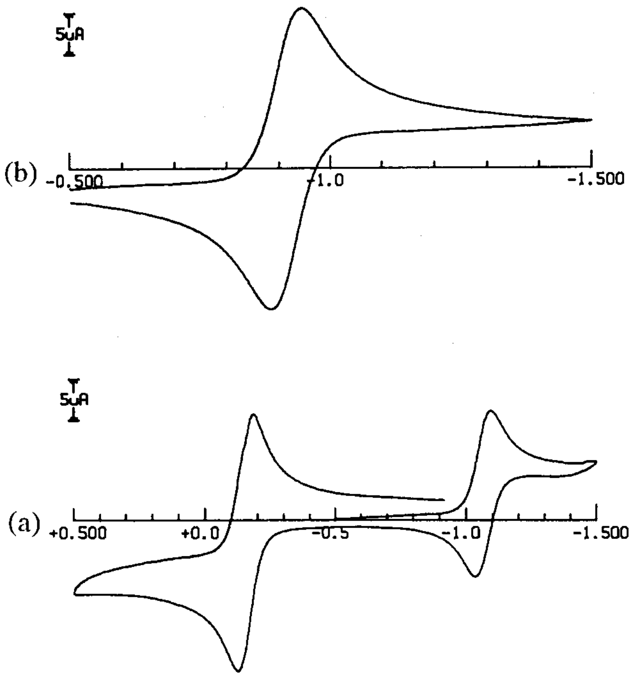

Fig. 2. Cyclic voltammetric responses recorded at a platinum electrode on CH_2Cl_2 solutions containing [*N*-Bu$_4$][PF$_6$] (0.2 mol dm^{-3}) and: (a) equimolar amounts (1.0×10^{-3} mol dm^{-3}) of **2**$^+$ and [(Me$_5$C$_5$)$_2$Fe]; (b) **5**$^+$ (1.6×10^{-3} mol dm^{-3}). Scan rate 0.05 Vs^{-1}.

Fig. 2(a) compares the responses of equimolar amounts of **2**$^+$ and [(Me$_5$C$_5$)$_2$Fe].

Both the monocations undergo reversibly the expected one-electron reduction to the neutral congeners [19]. As a matter of fact, controlled potential coulometric tests performed on the cathodic step of both the complexes showed the consumption of one electron per molecule. In both cases the exhaustively electrogenerated complexes **2** and **5** display cyclic voltammograms quite complementary to those shown in Fig. 2, thus confirming the chemical reversibility of the **2**$^+$/**2** and **5**$^+$/**5** redox couples. The analysis of the cyclic voltammograms with scan rate [20] proves that the two cathodic processes are electrochemically reversible too, thus allowing us to assume that no significant geometric reorganization takes place upon the electron exchange. The electrochemical parameters are compiled in Table 1.

Table 1
Electrochemical data for complexes **2**$^+$ and **5**$^+$ in dichloromethane solution

Complex	$E^{\circ\prime}_{+/0}$		ΔE_p (mV)[a]
	(V vs. SCE)	(V vs. Fc$^+$/Fc)	
2$^+$	−1.06	−1.44	67
5$^+$	−0.91	−1.27	65
[Co(C$_5$H$_5$)$_2$]$^+$	–	−1.36[b]	–

[a] Measured at 0.2 Vs^{-1}.

[b] From Ref. [21].

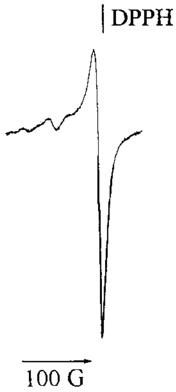

Fig. 3. X-band first-derivative EPR spectrum recorded at 100 K on a CH_2Cl_2 solution of **2**.

Because of the electron-donating ability of the *tert*-butyl substituents, $\mathbf{2}^+$ reduces at potential values somewhat more negative than those of unsubstituted cobaltocenium ion [21].

In view of the chemical reversibility of the $\mathbf{2}^+/\mathbf{2}$ and $\mathbf{5}^+/\mathbf{5}$ redox changes, we decided to examine the spectroscopic properties of the paramagnetic species **2** and $\mathbf{5}^+$, electrogenerating them by controlled potential electrolysis at −20°C. Fig. 3 shows the low-temperature ($T=100$ K) X-band EPR spectrum of **2**.

The intense and narrow absorption displays an $S=1/2$ signal with poorly resolved axial structure ($g_{\|} > g_{\perp} \neq g_{\mathrm{electron}} = 2.0023$) without the common resolution in the cobalt nucleus hyperfine splitting (I–Co = 7/2, natural abundance = 100%), as happens in the presence of weak electron spin/nuclear spin magnetic interaction [22]. The relevant best-fit computed parameters [23] are indicative of a significant metal orbital contribution to the actual SOMO: $g_{\|} = 2.028(5)$, $g_{\perp} = 2.004(5)$; $<g> = (g_{\|} + 2g_{\perp})/3 = 2.012(5)$.

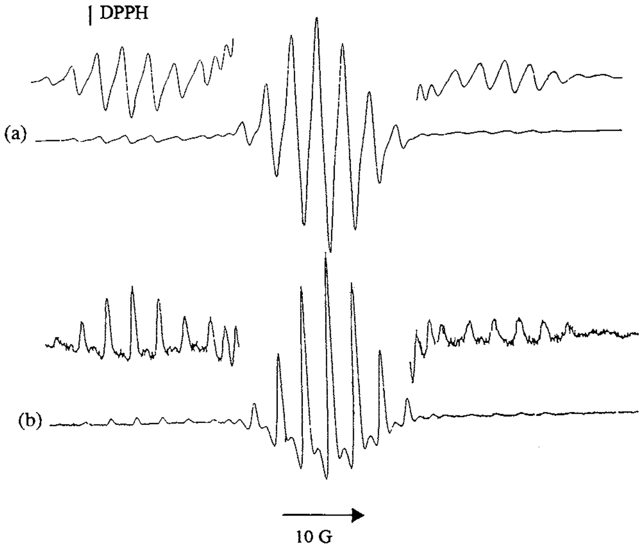

Fig. 4. X-band EPR spectra of a CH_2Cl_2 solution of $\mathbf{5}^+$ at different temperatures: (a) $T=100$ K; first derivative; bottom: second derivative; (b) $T=298$ K; top: first derivative; bottom: second derivative.

The noticeable difference between the g_{aniso} and g_{electron} values is attributable to the magnetic interaction of the $S=1/2$ unpaired electron with the cobalt nucleus.

Increasing the temperature at the glassy–fluid transition causes the anisotropic signal to drop out and the fluid solution exhibits a few minor spurious isotropic signals, which testify that **2** undergoes, as expected on the basis of its low reduction potential, chemical complications in the presence of traces of air. As a matter of fact, refreezing the solution does not allow the original signal to be recovered.

Fig. 4(a) shows the low-temperature ($T=100$ K) first-derivative X-band EPR spectrum of **5**, typical for a $S=1/2$ unpaired electron species.

As confirmed by the second-derivative profile (not shown), the intense narrow signal exhibits a slightly axial structure ($g_{\|} > g_{\perp} \neq g_{\mathrm{electron}} = 2.0023$), the lineshape analysis of which can be suitably carried out in terms of an $S=1/2$ electron spin Hamiltonian. Also in this case, no resolution of the typical satellite splitting of the Cr^{53} isotope (Cr^{53}; I = 5/2, natural abundance = 9.6%) is detected. The best-fitted paramagnetic parameters are: $g_{\|} = 1.993(5)$, $g_{\perp} = 1.982(5)$; $<g> = (g_{\|} + 2g_{\perp})/3 = 1.986(5)$.

Increasing the temperature at the glassy–fluid transition, the anisotropic profile drops out and the signal becomes isotropic, exhibiting a complex multiplet structure. At $T=200$ K, the isotropic absorption displays two main and well-resolved sets of multiplet signals, partially overlapped and in the intensity ratio of 1:15. Increasing the temperature, a third low-intensity multiplet appears at high field. At higher temperature, the intensity of the last signal significantly increases. This spectral behavior is quantitatively reversible with T. Fig. 4(b) shows the room-temperature X-band EPR spectrum of **5**, either in first-derivative or second-derivative form.

The best-fit EPR parameters characterize the three different paramagnetic species (hereafter indicated as l, m, and h, respectively): $g_{\mathrm{iso}}(\mathrm{l}) = 2.0004(5)$; $g_{\mathrm{iso}}(\mathrm{m}) = 1.9835(5)$; $g_{\mathrm{iso}}(\mathrm{h}) = 1.9673(5)$; $a_{\mathrm{iso}}(\mathrm{l}) = 3.6(5)$ G: $a_{\mathrm{iso}}(\mathrm{m}) = 3.7(5)$ G; $a_{\mathrm{iso}}(\mathrm{h}) = 3.6(5)$ G. $I(\mathrm{l}) = 2.0(2)$; $I(\mathrm{m}) = 63.7(2)$; $I(\mathrm{h}) = 1.0(2)$.

The different absolute spectral intensities I are evaluated in terms of $I = (\Delta H_{\mathrm{iso}})^2 h$, where ΔH_{iso} is the actual isotropic linewidth and h the height of the most intense central line of each paramagnetic species [22].

Interestingly, the central line (g_{iso} value) of the most intense medium signal fits well the $<g>$ value of the low-temperature absorption, suggesting that the spectrum recorded in frozen solution is mainly constituted by such a species. The three absorption patterns in fluid solution display the identical relative spectral multiplicity with slight difference in the relevant ΔH_{iso}, and they likely arise from the hyperfine interaction of the $S = 1/2$ unpaired electron with the eight magnetically equivalent $I = 1/2$ phenyl ring protons (H-1, $I = 1/2$; spectral nonuplet, with relative intensity ratios = 1:8:28:56:70:56:28:8:1). This spectral behavior clearly indicates that the corresponding SOMOs of the three multiplets are basically H_{1s} contributed with a minor involvement of the Cr_{3d} orbitals, as the Δg_{iso} difference between the g_{iso} and $g_{electron}$ values testify. Here, an upper limit for the Cr^{53} satellite hyperfine interaction can be stated: ΔH_{iso} (70 line) = 1.5 G $\geq a_{iso}(Cr)/5$. The data can be interpreted assuming the concomitant presence of three paramagnetic isomers, the nature of which mainly depends on the mutual position of the two huge *tert*-butyl residues in the phenyl ring. It is well conceivable that the most abundant paramagnetic species might be constituted by the isomer in which the rings assume the staggered conformation.

3. Conclusions

It is shown that bulky, sterically highly demanding aromatic ligands 1,4 di-*tert*-butylbenzene and 1,2,4, tri-*tert*-butyl-cyclopentadien-1-yl can be introduced as ligands in Cr and Co sandwich complexes employing different synthetic strategies. 1,4 Di-*tert*-butyl benzene forms a regular sandwich-type structure when co-condensed with chromium atoms in a 3:1 ratio. However, arene chromium triple decker complexes are not isolated from this metal atom reaction. This contrasts with co-condensation experiments with Cr and the 1,3,5 tri-*tert*-butyl benzene ligand. The trianion of the polycondensed hydrocarbon decacyclene reduces the chloro bridged dinuclear cobalt complex **7** to give the cobaltocene **2**. The two complexes $\mathbf{2}^+$ and $\mathbf{5}^+$ display a rather similar redox aptitude, namely, a reversible one-electron reduction to the corresponding neutral congeners that occurs at rather similar potential values (around −1 V, versus SCE). Nevertheless, the EPR spectra of their neutral species **2** and **5** show that the LUMOs of the two species are significantly different in nature: the LUMO of $\mathbf{2}^+$ is essentially metal based, whereas that of $\mathbf{5}^+$ is essentially ligand based.

4. Experimental

4.1. General information

Metal atom reactions were conducted in custom-built all-glass static metal vapor reactors based on the design published by Klabunde [24] Chromium metal was 99.9% pure and was used as chips (Balzers, Lichtenstein). Metal sublimation was from heated tungsten alumina crucibles (Mathis, CA, USA) which were wrapped with alumina wool to compensate heat loss. In our set up of the metal vapor reactor an amount of approximately 20% of metal is not introduced into the reaction zone of the metal/ligand co-condensate. 1,4 di-*tert*-Butylbenzene and decacyclene are commercially available (Aldrich). Decacyclene was sublimed in vacuo prior to use. 1,2,4 tri-*tert*-Butyl Cp was prepared according to the literature [25]. Except the metal vapor synthesis, all reactions were carried out under an atmosphere of dry nitrogen gas with standard Schlenk techniques. Microanalyses were performed by the microanalytical laboratory of the Chemistry Department of the University/GH-Essen. All solvents were dried following standard methods and were stored under nitrogen. The NMR spectra were recorded on a Bruker AC 300 spectrometer (300 MHz for ^1H, 75 MHz for ^{13}C) and referenced against the remaining protons of the deuterated solvent used. NMR samples were prepared by vacuum transfer of predried, degassed solvents onto the appropriate amount of solid sample, followed by flame sealing of the NMR tube. MS spectra were recorded on a MAT 8200 instrument using standard conditions (EI, 70 eV) and the fractional sublimation technique for compound inlet. Material and apparatus for electrochemistry and coupled EPR measurements have been described elsewhere [26]. All the potential values are referred to the saturated calomel electrode (SCE). Under the present experimental conditions, the one-electron oxidation of ferrocene occurs at $E^{\circ\prime} = +0.38$ V. The external magnetic field H_0 for X-band ($\nu = 9.44$ GHz) was calibrated by using a DPPH powder sample ($g_{DPPH} = 2.0036$).

4.2. Bis(η^5-1,2,4-tri-tert-butyl-Cp)Co **2**

Decacyclene (500 mg, 1.1 mmol) were suspended in 100 ml THF and transferred into a flask in which a thin mirror from 160 mg (4.0 mmol) potassium metal had been prepared. After 3 days ≈90% of the metal was dissolved, resulting in a deep red–brown solution. After cooling to −78°C, 1.1 g [{(η^5-1,2,4-tri-*tert*-butyl-Cp)CoCl}$_2$] **7** were added to this solution in one batch under stirring and the resulting mixture was warmed to room temperature (r.t.) during several hours. After removal of all volatiles, the residue was dissolved in diethylether and crystallized from that solvent at −30°C, resulting in 560 mg (1.06 mmol, 65%) shimmering brown to black crystals of **2**. MS (EI, 70 eV) [M^+] 525(100). ^1H-NMR (C_6D_6, 27°C) $\delta = 3.47$(s, 36H), 3.65(s, 18H). Anal. Calc. –$C_{34}H_{58}Co$ (525.78) C, 77.67; H 11.12; Found C, 78.59; H 10.56.

4.3. Bis(1,4-di-tert-butylbenzene)chromium(0) **5**

During 3 h, 5 g (28.6 mmol) 1,4-di-*tert*-butylbenzene were co-condensed with 0.52 g (10 mmol) chromium metal at −196°C. After warming up to r.t., the brown–

olive green co-condensate was dissolved in 100 ml of toluene and filtered to remove any excess metal. The deep green–brown solution was pumped to dryness and excess ligand removed by sublimation at 80°C/10^{-2} Pa. The brown residue was finally sublimed at 150°C/10^{-2} Pa giving **5** (420 mg, 1 mmol) as a greenish brown microcrystalline solid. Olive green crystals suitable for X-ray analysis could be obtained from a concentrated toluene solution at -30°C. ^{1}H-NMR (300 MHz, C_6D_6, 27°C): δ (ppm) = 4.44 (s, 8H, =CH), 1.34 (s, 36H, CH_3). ^{13}C-NMR (75 MHz, C_6D_6): δ (ppm) = 101.7 (=C*t*-Bu), 73.4 (=CH), 34.4 (*C*(CH_3)$_3$), 32.1 (C(CH$_3$)$_3$). IR (KBr): $\tilde{\nu} = 3058$ m (=CH), 2961 s (*t*-Bu), 1367 s (*t*-Bu), 1261 s (*t*-Bu). MS (EI, 70 eV) M^+ 432 (34); M^+ $-C_6H_4$(*t*-Bu)$_2$ 242(100); C_6H_4(*t*-Bu)[C(CH_3)$_2$]$^+$ 175 (10); Cr^+ 52 (35). Anal Calc. $-C_{28}H_{44}Cr$ (432.65) C 77.73; H 10.25; Found C 77.86; H 10.37.

5. Supplementary data

Crystallographic data for the structural analysis have been deposited with the Cambridge Crystallographic Data Centre, CCDC no. 119097. Copies of this information may be obtained free of charge from The Director, CCDC, 12 Union Road, Cambridge CB2 1EZ, UK [fax: +44-1223-336-033 or e-mail: deposit@ccdc.cam.ac.uk or http://www.ccdc.ac.-ac.uk].

Acknowledgements

J.J.S. thanks the Deutsche Forschungsgemeinschaft for a Heisenberg Fellowship, the Volkswagen Foundation and the Fonds der Chemischen Industrie for financial support. Thanks are also due to Dr D. Stöckigt and Dr K. Seevogel and their coworkers (MPI, Mülheim) for recording EI mass spectra and IR spectra. P.Z. gratefully acknowledges the financial support of University of Siena (ex-quota 60%).

References

[1] Ch. Elschenbroich, A. Salzer, Organometallchemie 2 (1988) 403.

[2] (a) P.L. Timms, Adv. Inorg. Radiochem. 14 (1972) 121. (b) M.J. Mc Glinchey, T.S. Tan, J. Am. Chem. Soc. 98 (1976) 2271. (c) N. Hao, M.J. Mc. Glinchey, J. Organomet. Chem. 161 (1987) 381. (d) E.B. Wilburn, P.S. Skell, J. Am. Chem. Soc. 104 (1982) 6989. (e) H. Brunner, H. Koch, Chem. Ber. 115 (1982) 65. (f) V. Graves, J.J. Lagowski, Inorg. Chem. 15 (1976) 577. (g) V. Graves, J.J. Lagowski, J. Organomet. Chem. 120 (1976) 397. (h) H. Ssekaalo, J.J. Lagowski, C.M. Seymour, Inorg. Chim. Acta 173 (1990) 237. (i) A. Yu, V.M. Aleksandrov, V.M. Fomin, A.V. Lunin, Kinetika i Kataliz 16 (1975) 618. (j) Ch. Elschenbroich, J. Schneider, H. Prinzbach, W.D. Fessner, Organometallics 5 (1986) 2091. (k) Ch. Elschenbroich, J. Koch, J. Schneider, B. Spangenberg, P. Schiess, J. Organomet. Chem. 317 (1986) 41. (l) Ch. Elschenbroich, J. Schneider, H. Mellinghoff, J. Organomet. Chem. 333 (1987) 37. (m) Ch. Elschenbroich, J. Schneider, M. Wünsch, J.L. Pierre, P. Barret, P. Chautemps, Chem. Ber. 121 (1988) 177. (n) Ch. Elschenbroich, J. Schneider, W. Massa, G. Baum, H. Mellinghoff, J. Organomet. Chem. 355 (1988) 163. (o) Ch. Elschenbroich, J. Schneider, H. Burdorf, J. Organomet. Chem. 391 (1990) 195. π-η^6-heteroarene examples: (p) Ch. Elschenbroich, M. Nowotny, B. Metz, J. Graulich, W. Massa, K. Biehler, W. Sauer, Angew. Chem. 103 (1991) 601; Angew. Chem. Int. Ed. Engl. 30 (1991) 547. (q) E.J. Wucherer, E.L. Muetterties, Organometallics 6 (1987) 1691. (r) Ch. Elschenbroich, J. Koch, J. Kroker, M. Wünsch, W. Massa, G. Baum, G. Storck, Chem. Ber. 121 (1988) 1983. (s) Ch. Elschenbroich, F. Bär, E. Bilger, D. Mahrwald, M. Nowottny, B. Metz, Organometallics 12 (1993) 3373. (t) Ch. Elschenbroich, J. Kroker, M. Nowotny, A. Behrendt, B. Metz, K. Harms, Organometallics 18 (1999) 1495. (u) Ch. Elschenbroich, J. Kroker, W. Massa, M. Wünsch, A.J. Ashe, Angew. Chem. 98 (1986) 562; Angew. Chem. Int. Ed. Engl. 25 (1986) 571.

[3] (a) F.G.N. Cloke, M.F. Lappert, G.A. Lawless, A.C. Swain, J. Chem. Soc. Chem. Commun. (1987) 1667. (b) J.G. Brennan, F.G.N. Cloke, A.A. Sameh, A. Zalkin, J. Chem. Soc. Chem. Commun. (1987) 1668. (c) F.G.N. Cloke, K.A.E. Courtney, A.A. Sameh, A.C. Swain, Polyhedron 8 (1989) 1641.

[4] (a) P.L. Timms, Adv. Inorg. Radiochem. 14 (1972) 212. (b) J.J. Schneider, Habilitation Thesis, University of Essen, 1993.

[5] J.J. Schneider, U. Specht, R. Goddard, C. Krüger, Chem. Ber. Recueil 130 (1997) 161.

[6] J. Okuda, J. Organomet. Chem. 385 (1990) C39.

[7] J. Okuda, J. Organomet. Chem. 367 (1989) C1.

[8] H. Sitzmann, G. Wolmershäuser, Z. Naturforsch. 52b (1997) 398.

[9] H. Sitzmann, M. Schär, E. Dorrmann, M. Kelemen, Z. Anorg. Allg. Chem. 623 (1997) 1609.

[10] (a) W.N. Lamanna, J. Am. Chem. Soc. 108 (1986) 2096. (b) W.N. Lamanna, W.B. Gleason, D. Britton, Organometallics 6 (1987) 1583.

[11] Ch. Elschenbroich, U. Zenneck, J. Organomet. Chem. 160 (1978) 125.

[12] S.E. Anderson Jr., R.S. Drago, J. Am. Chem. Soc. 92 (1970) 4244.

[13] K.H. Hausser, H. Brunner, J.C. Jochims, Mol. Phys. 10 (1966) 253.

[14] (a) G.M. Sheldrick, SHELXS-86, Program for Crystal Structure Solution, Universität Göttingen, 1986. (b) G.M. Sheldrick, SHELXL-93, Program for Crystal Structure Refinement, Universität Göttingen, 1993.

[15] G.A. Orpen, in: A.J.C. Wilson (Ed.), Int. Tab. Cryst, vol. C, Kluwer, Dordrecht, 1992, p. 729.

[16] Decacylene is known to consume between 2.3 and three equivalents of postassium metal. L.B. Ebert, G.E. Milliman, D.R. Millis, J.C. Scanlon, Adv. Chem. Ser. 217 (1988) 109.

[17] J.J. Schneider, U. Specht, Z. Naturforsch 50b (1995) 684.

[18] J.J. Schneider, C. Krüger, Chem. Ber. 125 (1992) 843.

[19] D. Astruc, Electron Transfer and Radical Processes in Transition-Metal Chemistry, Wiley–VCH, New York, 1995 Chapter 2.

[20] E.R. Brown, J.R. Sandifer, in: B.W. Rossiter, J.F. Hamilton (Eds.), Physical Methods of Chemistry. Electrochemical Methods, vol. 2, Wiley, New York, 1986 Chapter 4.

[21] R.S. Stojanovic, A.M. Bond, Anal. Chem. 65 (1993) 56.

[22] F.E. Mabbs, D. Collison, Studies in Inorganic Chemistry. Electron Paramagnetic Resonance of d Transition Metal Compounds, Elsevier, New York, 1992 Chapter 16.

[23] (a) J.P. Lozos, B.M. Hoffman, C.G. Franz, QCPE (1974) 259. (b) G. Della Lunga, ESRMGR Simulation Program, 1998.

[24] K.J. Klabunde, Acc. Chem. Res. 8 (1975) 393.

[25] (a) E.V. Dehmlow, C. Bollmann, Z. Naturforsch. 48b 1993 457. (b) C.G. Vernier, E.W. Casserly, J. Am. Chem. Soc. 112 (1990) 2808.

[26] P. Zanello, F. Laschi, M. Fontani, C. Mealli, A. Ienco, K. Tang, X. Jin, L. Li, J. Chem. Soc. Dalton Trans. (1999) 965.